



Determination of caved and water-conducting fractured zones of “two soft and one hard” unstable coal seam

Yang Chen^{1,2} · Shuyun Zhu^{1,2}

Received: 7 March 2020 / Accepted: 15 June 2020 / Published online: 25 June 2020
© Akadémiai Kiadó 2020

Abstract

The height of the development of a caved zone (CZ) and a water-conducting fractured zone (WCFZ), hereinafter “CZ and WCFZ”, in mining of soft coal with a soft mine floor, hard mine roof and different thicknesses of the coal seam, hereinafter “two soft and one hard” unstable coal seam, is of interest in the long wall coal mining. An observation borehole was drilled above a coal seam with an average thickness of 4.0 m. By using borehole imagery technique and comparing the borehole images at different distances from the working face, the height of “CZ and WCFZ” at the working face is calculated under the condition of insufficient mining. Based on field observations, a 3D numerical model is developed under the condition of full mining, the height of CZ is calculated to be 14.4 m and the height of WCFZ calculated to be 67.0 m. The numerical model also shows changes in the vertical stresses in the overburden strata above the roof of the coal seams and it is related to the development of the “CZ and WCFZ”. At the same time, based on the key strata theory and multiple linear regression, the height of WCFZ in the working face of this case study is predicted to be 67.0 m and 64.8 m respectively, which is close to the numerical simulation results. At the same time, 30 groups of measured data are collected to analyze the main factors affecting the WCFZ, and the influence of different lithology characteristics of overburden strata on the WCFZ is mainly discussed. The results show that the height of WCFZ is hard–hard > hard–soft > soft–hard. The results provide important practical guidelines for the prevention and control of roof water hazards in coal mine thus improving the safety of mining.

Keywords Water-conducting fractured zone height · Borehole imaging · Numerical simulation · Key stratum · Lithology characteristics of overburden strata

List of symbols

CZ Caved zone

✉ Shuyun Zhu
4726@cumt.edu.cn

¹ Key Laboratory of Coalbed Methane Resources and Reservoir Formation Process of the Ministry of Education, China University of Mining and Technology, Xuzhou 221116, Jiangsu Province, People's Republic of China

² School of Resources and Geosciences, China University of Mining and Technology, Xuzhou 221116, Jiangsu Province, People's Republic of China

WCFZ H_{ii}	Water-conducting fractured zone
k_p	Fragmentation coefficient
h_i, h_n	Thickness
r_i	Bulk density
E_i	Elastic modulus
$q_i(X)_n$	Load of the n th hard rock stratum on the first hard rock stratum
l_n	Limited span
σ_n	Tensile strength
q_n	Load of the n th hard rock stratum
n	Total number of rock layers
L_n	Broken distance
H_n	Distance of the hard rock stratum at the n th stratum from the upper surface of coal seam
γ	Average broken angle of the rock stratum
Δs	Maximum subsidence of broken block in main key stratum
M	Thicknesses of the mined seam
h	Distance between main key stratum and top of coal seam
k	Opening of crack in main key stratum
s	Thickness of the main key stratum
L	Broken block length
β	Opening angle between the broken block and the key stratum
α	Change in angle before and after the broken block
l_{zn}	Periodic weighting step
L_x	Width of the working face

1 Introduction

With increases in mining activities in worldwide, the threat of water inrush in underground mining is becoming more and more serious (Chen et al. 2019a, b; Zeng et al. 2020; Huang et al. 2018, 2019; Wu et al. 2020). Due to secondary stress concentration and stress redistribution after mining, deformation and failure of the roof will inevitably occur. Failure of the roof creates “three zones” (Guo et al. 2019; Zhang et al. 2014; Liu et al. 2019b) which are the caved zone (CZ), water-conducting fractured zone (WCFZ) and bending zone. Among them, “CZ and WCFZ” is the main failure zone that is directly related to the overlying aquifer, i.e. the so-called “CZ and WCFZ” problem. WCFZ has interconnecting fissures in the rock mass which provide water conducting passages for water to flow into the mine. The height of the WCFZ can be considered as an index that reflects the water-conducting characteristics of rock mass after failure (Liu et al. 2015; Su and Yue 2017; Liu et al. 2018). The height of the “CZ and WCFZ” formed after deformation and removal of the overlying coal strata has much impact on the safety of mines. It is evident that once the WCFZ is connected to a water source, water may flow to the working face, which may cause flooding accidents (Majdi et al. 2012; Miao et al. 2011; Wu et al. 2017; Li et al. 2018; Szokoli et al. 2018). Therefore the height of the “CZ and WCFZ” plays an important role in the assessment of hazards caused by water in the mine (Wang et al. 2016; Zhang et al. 2018a; Guo et al. 2012). Moreover, determining the height of the “CZ and WCFZ” provides an important assessment of the safety of mines to form the basis in finding the upper limits of mining the coal seam which can prolong the service life of the

mine in selecting the type of roof support for optimum efficiency in mining coal resources. In general, accurate calculation of the height of the “CZ and WCFZ” is the key in the prediction and prevention of sudden water inrush from the roof of the mine. Such an analysis also provides the scientific basis for safe mining designs for mines under buildings and railways and mining through water bodies and for the retention of waterproof coal pillars (Chen et al. 2019a; Liu et al. 2019a; Zhang et al. 2009; Fan and Ma, 2018; Nan et al. 2017). WCFZ is caused by coal seam mining, and the development of WCFZ is related to the fracture movement of the geological strata. Fracture movement is controlled by key stratum which affect the development of the WCFZ. Therefore, the height of the WCFZ can be determined by identifying the key stratum in the overburden strata (Zhang et al. 2018b).

At present, there are mainly empirical formulas (Miao et al. 2011; Liu et al. 2015), field measurements (Chen et al. 2019a; Miao et al. 2011; Zhang et al. 2018b) and numerical simulations (Chen et al. 2019a; Guo et al. 2019; Li et al. 2018; Liu et al. 2015; Liu et al. 2018) used to determine the height of WCFZ. However, field measurements are the most direct and effective way to obtain the height of the “CZ and WCFZ”, and also the field data for validation purposes in basic research. Field measurements, which mainly include borehole imagery (Chen et al. 2019a; Li et al. 2018; Liu et al. 2018), pressurized water permeability tests (Miao et al. 2011; Li et al. 2018; Zhang et al. 2018b) and geophysical logging (Li et al. 2018). Each of these techniques has its advantages and disadvantages in obtaining underground information of the strata. According to actual field conditions of the working face, the literature has selected the borehole imagery technique to determine the height of the “CZ and WCFZ”. In addition, a numerical model has been used to analyze the field data and gain a better understanding of the field measurements. Finally, the height of the WCFZ can be calculated, and the height and characteristics of the WCFZ can be analyzed by identifying the key stratum and multiple linear regression. Findings from this research provide a method in predicting water hazards of the roof and effective management of roof support for mines at the working face.

2 General condition of Working Face 23301

Working Face 23301 is located in the west wing of the No. 23 mining district, with the goaf of Working Face 23300 to the north, and an unmined coal seam of Working Face 23303 to the south. The end of the mine is located east of Working Face 23301 with a narrow coal belt to the west. The ground surface landscape of the mine is mainly hilly with some small hills. Below the vegetation at the ground surface lies a layer of quaternary loess deposits with a thickness of between 1 and 5 m. The ground elevation of the working face is between 322 and 423 m above sea level and the height of the working face is between 2.1 and 99.0 m, coal seam with an average thickness is 4.0 m. The working face has a strike length of about 1126 m, a width of about 133 m and an area of about 149,710 m². The strike of the coal (rock) stratum is NE35–42°, and the dip direction is SE55–48°, with an inclination angle of 11°–30°, and an average inclination angle of 17°. There are eleven faults in the working faces of the No. 23 mining district, with a minimum dip of 1.2 m and a maximum dip of 7.8 m of the fault planes. There is one fault with a dip of more than 5 m, three faults with a dip of 3–5 m and seven faults with a dip of less than 3 m of the fault planes. According to the distribution of thickness of the No. II₁ coal seam exposed at the working face and surrounding borehole information (Fig. 1), the maximum thickness of the

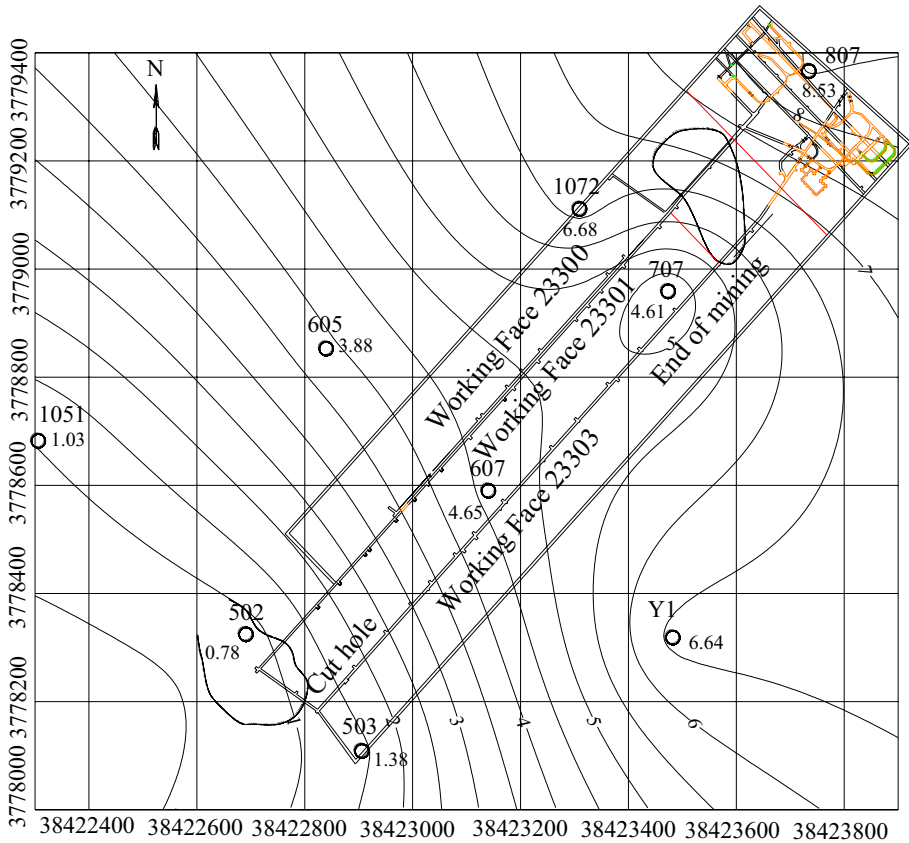


Fig. 1 Contour of thickness of No. II₁ coal seam at and around Working Face 23301 (unit: m)

coal seam from the non-mined areas near the cut hole to the end of the mining can reach more than 7 m. The thickness of the coal seam varies greatly at this location.

3 Field measurement

3.1 Basic approach and testing procedures

Borehole imagery of the in situ conditions of the rock before mining was carried out near the working face. Without interfering with the mining activities, a borehole was selected at a location ahead of the working face in the direction of the mining. When the working face was far away from the borehole, the characteristics of borehole wall were measured. With the advancement of the working face, changes in the characteristics of the rock that surrounded the borehole can be measured from the borehole. Therefore, the deformation of the rock could be analyzed for different locations of the working face during mining by measuring the changes in the surface characteristics of the borehole wall from the down-hole imagery. The height of the “CZ and WCFZ” could be determined based on the measurements in the borehole. Borehole wall imagery was carried out by using a V8-3188DK

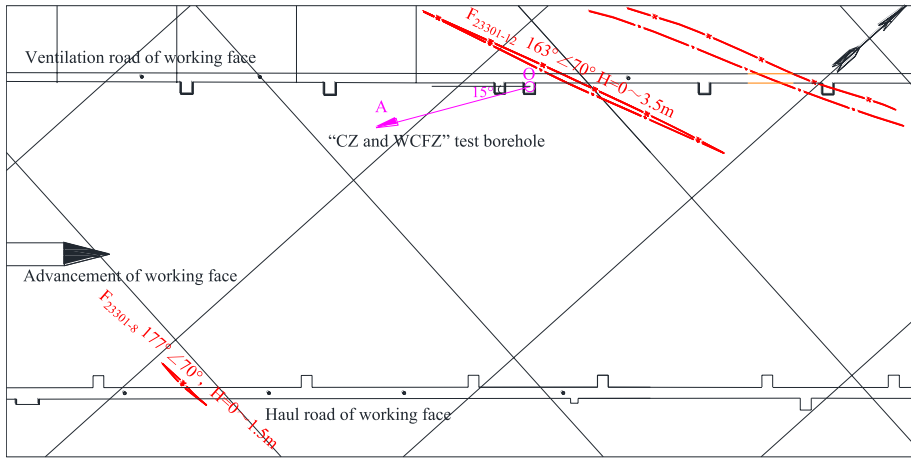
inspection system as shown in Fig. 2. Pictures of the rock in the borehole are displayed on an LCD screen at different detection depths and time. Subsurface geological layers, rock fractures and fracture widths can be captured by the camera in real time. The images can be processed by using related software to provide more information on the underground conditions (Jia et al. 2000). The layout of the borehole for measuring the height of the “CZ and WCFZ” is shown in Fig. 3. Figure 3a shows the plan sketch layout of borehole location and Fig. 3b shows the borehole layout section. The borehole parameters are summarized in Table 1. Due to field limitations, three sets of measurements were carried out. At the beginning of each measurement, video recording was carried out at a basically constant camera speed. The speed of the camera was slowly increased. Deformation and failure to the rock were captured by the camera at different depths. The deformation, fractures and failure of the rock could be determined through image analysis of the rock in three separate recordings and comparative analysis of the images at different depths. Since a large number of images were obtained in each measurement, only a few images that are related to the determination of the height of the “CZ and WCFZ” is presented here; see Figs. 4 and 5.

3.2 Measured results and analysis

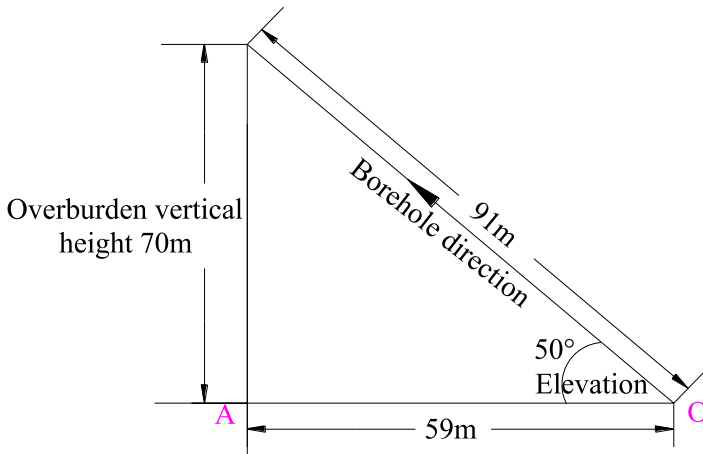
The height of the “CZ and WCFZ” was estimated by conducting a comprehensive comparative analysis of the deformation and failure images of the borehole wall at different depths and different distances from the working face. On October 8, 2018, November 8, 2018 and December 30, 2018, three field measurements of the height of the “CZ and WCFZ” of roof overburden borehole was carried out. As shown in Fig. 4, the borehole images show that there are obvious differences in the borehole surface instabilities and deformations in the direction of the borehole at a location about 9.4 m away from the borehole orifice. The third measurement shows that there is clear evidence of borehole wall collapse with obvious cracks at this location, which are not observed in the

Fig. 2 V8-3188DK inspection system





(a) Plan sketch layout of borehole location



(b) Schematic diagram of borehole layout section

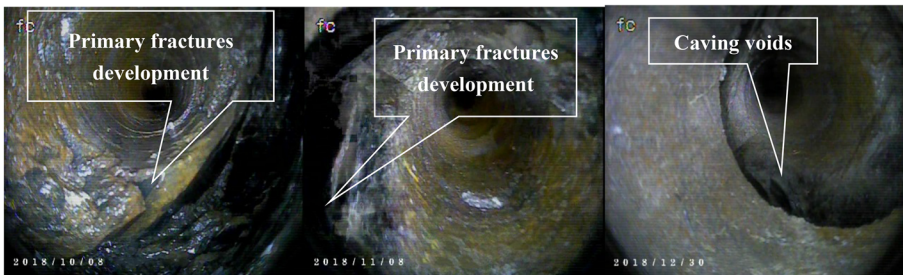
Fig. 3 Schematic of borehole layout

previous images. In addition, the three images obtained at 9.2 m and 9.6 m during the third measurement clearly reflect the differences in the three images at different times (Fig. 4a, b), thus suggesting that the CZ has developed to a distance of 9.4 m along the borehole.

The third test along the direction of the borehole shows obvious differences in the fracture deformation at a location of about 50.0 m away from the borehole orifice. There are obvious cracks and spalling of the borehole wall that are not detected in previous images (Fig. 5). In addition, in the third measurement, it was found that the three images at a location between 49.8 and 50.2 m show clear differences in the images at different times (Fig. 5a, b). Therefore, the WCFZ has been developed to a distance of 50.0 m

Table 1 Borehole parameters

Technical parameter	“CZ and WCFZ” test borehole
Diameter of borehole opening (mm)/depth (m)	146/6.0
Diameter of borehole orifice of borehole pipe (mm)/length (m)	127/5.0
Diameter of borehole (mm)	108
Borehole orientation (°)	207
Inclination of borehole (°)	50
Angle of haul road (°)	15
Borehole depth (m)	91
Horizontal projection distance of borehole depth on working face (m)	59
Overburden height (m)	70



(1) First measurement

(2) Second measurement

(3) Third measurement

(a) Height of the CZ (9.4 m away from the borehole orifice, corresponds to a vertical height of 7.2 m)



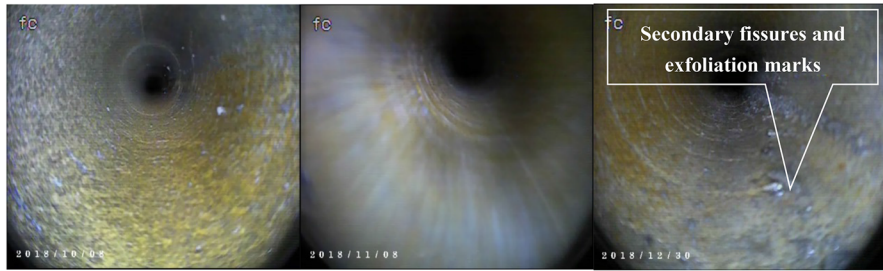
(1) First measurement

(2) Second measurement

(3) Third measurement

(b) 9.6 m from the borehole orifice, corresponds to a vertical height of 7.4 m

Fig. 4 Comparative image analysis of the borehole wall and surrounding rock in the CZ (first, second and third measurements were taken on Oct 8, 2019, Nov 8, 2018 and Dec 30, 2018 respectively)



(1) First measurement (2) Second measurement (3) Third measurement

(a) Height of the WCFZ (50.0 m away from the borehole orifice, corresponds to a vertical height of 38.5 m)



(1) First measurement (2) Second measurement (3) Third measurement

(b) 50.2 m from the borehole orifice, corresponds to a vertical height of 38.6 m

Fig. 5 Comparison image analysis of the measured borehole wall and surrounding rock in the WCFZ (first, second and third measurements were taken on Oct 8, 2018, Nov 8, 2018 and Dec 30, 2018 respectively)

along the borehole. On December 30, 2018, the top of the CZ was about 9.4 m from the borehole orifice, and the top of the WCFZ was about 50.0 m from the borehole orifice.

The height of the “CZ and WCFZ” was roughly estimated after conducting a comparative analysis of the borehole images at different times. The results showed that the height of the CZ is about 7.2 m, and the height of the WCFZ is about 38.5 m; see Fig. 3b.

Note: the height of the “CZ and WCFZ” measured on site is 5 m ahead of the horizontal distance of the working face pushed to the borehole. Due to the limitation of the site conditions, the test borehole is set in the middle of the 23301 ventilation road of working face, so the measurement results after the working face pushed can not be carried out. Theoretically, this kind of measured height is only the height of the WCFZ and CZ under the condition of insufficient caving, which should be less than the height of the WCFZ and CZ fully caving after the mining of the working face.

4 Numerical simulation of Working Face 23301

4.1 Model development

According to field observations during mining and the borehole data, the subsurface rock strata in the studied area can be divided into 10 geological formations according to

lithology and integrity, including limestone, mudstone, marl, sandy mudstone, siltstone, carbonaceous mudstone, coal (from the No. II₁ coal seam), and medium, fine and coarse grained sandstone. There are 27 layers from bottom to top. The thickness of the layer of coal (No. II₁ coal seam) under the “CZ and WCFZ” borehole is equal to 4 m. The geological profile along the strike direction is shown in Fig. 6.

A 3D coordinate system was then established by considering the coal seam floor as the coordinate origin. The bottom surface of the coal seam formed the XOY plane with the inclined horizontal projection direction as the positive Y direction, the coal seam trend as the X direction, and the vertical plane as the positive Z direction. Based on actual mining conditions, the model simulated a block of 200 m × 120 m, which includes the test borehole, with a height of 107 m.

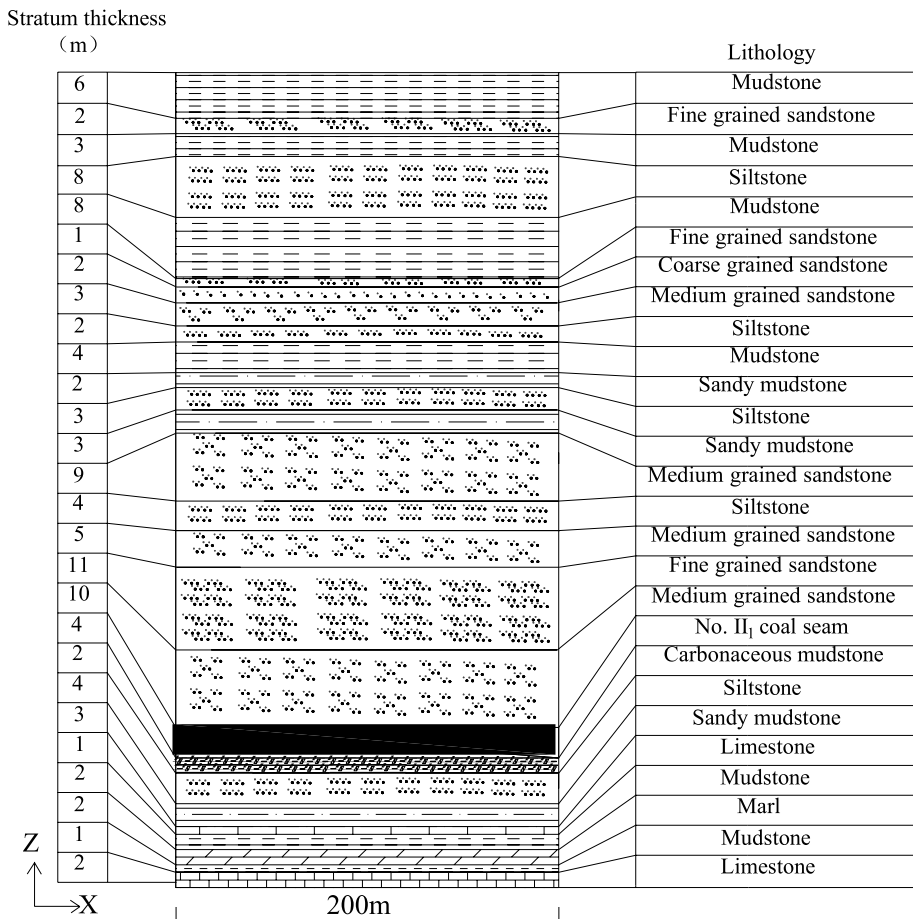


Fig. 6 Geological profile of the mine

4.2 Boundary conditions and physical and mechanical parameters

The boundary conditions for numerical modeling are defined in this section as follows:

- (1) The vertical geostatic stress of the overlying strata is modelled by applying a uniformly distributed load on the top boundary of the model based on the self-weight of the rock and soil.
- (2) The rock and soil strata are assumed to be homogeneous continua.
- (3) The original stress field is considered as a gravity stress field, and the effect of the tectonic stress field is not considered.

The boundary conditions and initial conditions of the model are shown in Fig. 7. All vertical boundaries of the model are fixed in the horizontal direction but free to move in the vertical direction. The bottom boundary is constrained in all directions. The top boundary is subjected to a uniform load of 5.85 MPa due to the self-weight of a 234 m thick overburden (based on a stress rate of 0.025 MPa/m of overburden). Support coal pillars of 40 m are placed on both sides of the strike, and there are inclined pillars of 30 m on both sides of inclination, which are 120 m in mined length and 60 m in mined width.

The parameters of the rock and soil used in the model based on physical and mechanical laboratory tests on supplementary samples of the rock and soil are shown in Table 2. In order to better understand the field observations, a 3D numerical model was built by using FLAC^{3D} software based on the morphology of the rock formations and the height of the “CZ and WCFZ”. The model has 61,200 element blocks with 66,092 nodes.

4.3 Modeling results

After the completion of mining of the coal seam, the ground ahead of the working face has obvious yielded at the roof and floor; see Fig. 8. Specifically, shear yielding occurs at the edge of the roof of the working face, tension yielding occurs in the middle of the goaf, and

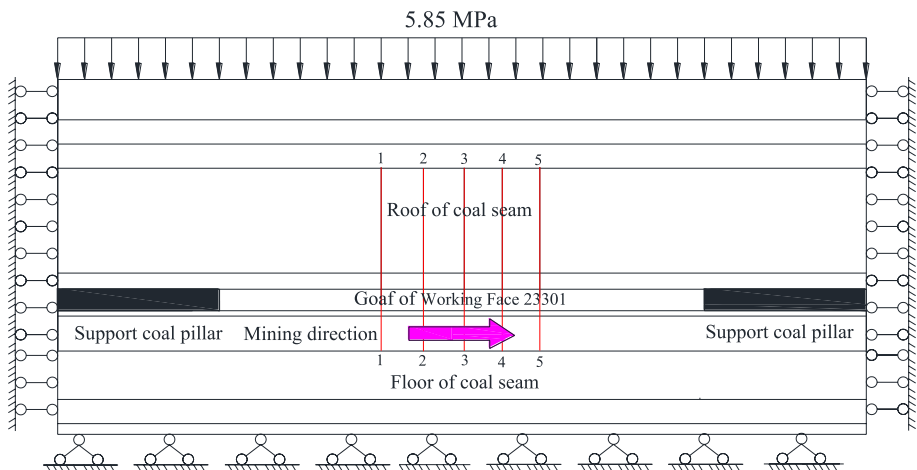


Fig. 7 Domain and boundary conditions of numerical model

Table 2 Physical and mechanical properties of roof and floor of mining district

Type of rock	Density ρ (Kg/ m ³)	Elastic modulus E (GPa)	Poisson's ratio ν	Cohesion c (MPa)	Internal friction angle φ (°)	Tensile strength σ_t (MPa)
Limestone	2720	11.9	0.19	10.80	40	3.21
Mudstone	2576	4.2	0.27	1.28	41	0.81
Marl	2648	8.1	0.21	5.04	36	2.01
Sandy mudstone	2562	4.8	0.26	2.01	43	1.42
Siltstone	2643	8.5	0.20	3.00	43	1.89
Carbonaceous mudstone	2243	3.4	0.24	1.51	46	1.13
No. II ₁ coal seam	1400	0.5	0.30	1.50	38	0.60
Medium grained sandstone	2692	9.7	0.19	3.71	48	2.10
Fine grained sandstone	2677	8.2	0.20	4.31	36	2.65
Coarse grained sandstone	2723	10.5	0.18	3.21	52	1.90

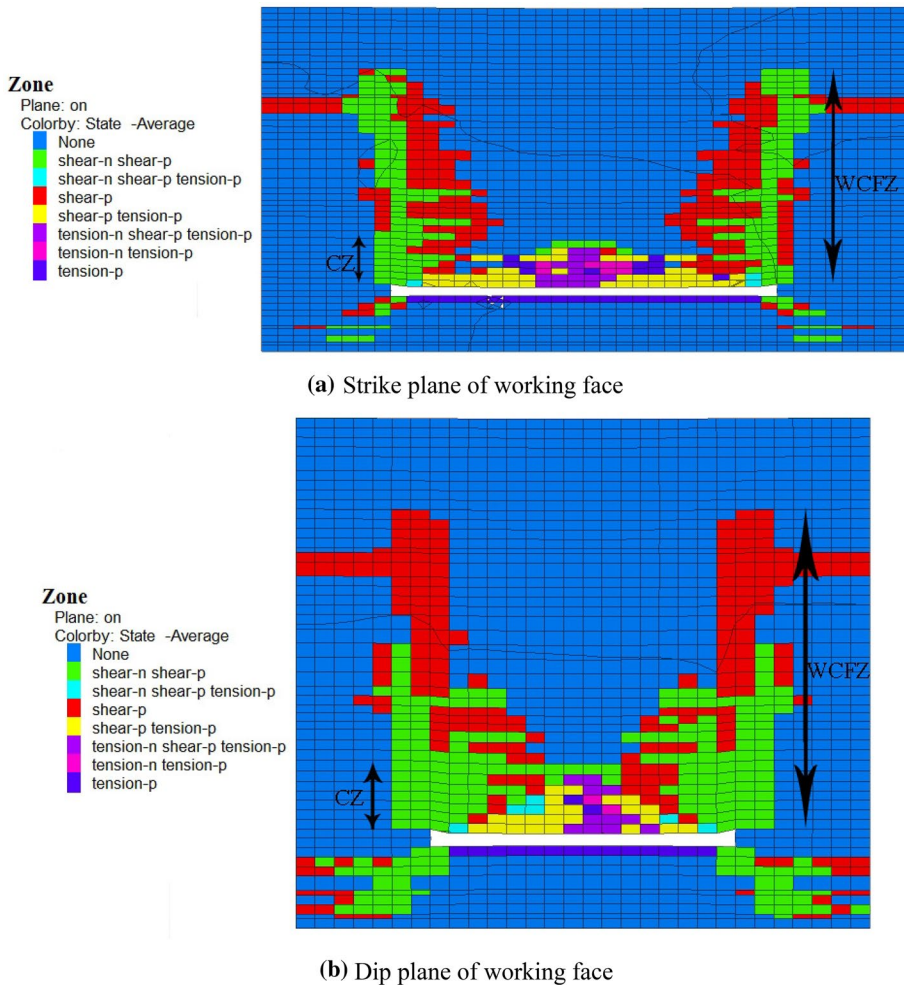
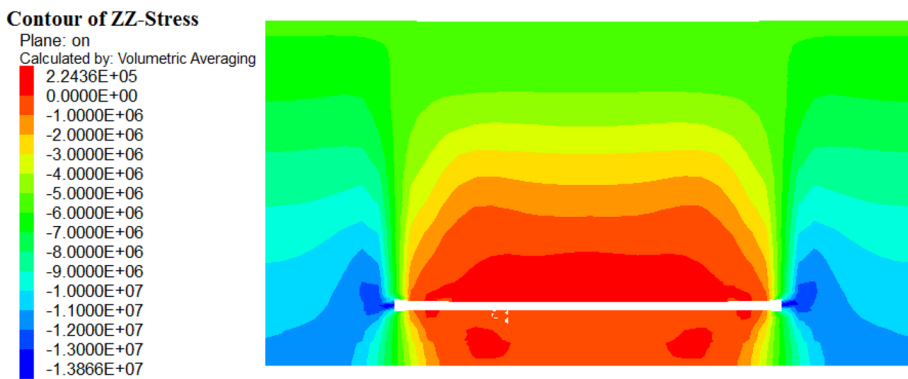


Fig. 8 Distribution of plastic zone ahead of working face

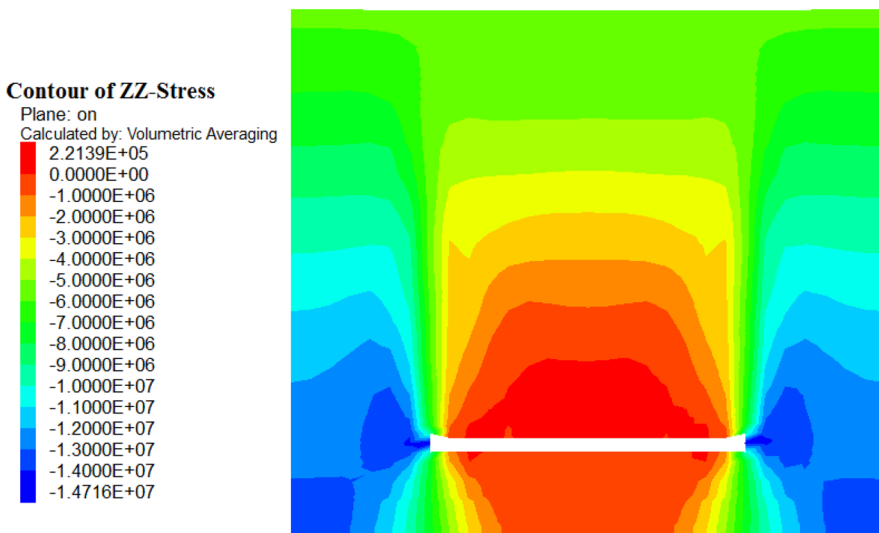
the yield/failure zone in the overlying strata immediately above the mine shows an irregular saddle shape. The height of the failure zone in the overlying strata is the highest at the upper part of the cut hole and the upper part of the end of the working face. The distribution of shear stress is basically symmetrical about the mid-perpendicular line of the strike of the working face or the center line of the model. Shear stress concentration occurs near the cut hole and end of the working face. Shear stress concentration is seen at locations where shear yield can easily occur, which leads to the formation of shear cracks and water conducting passages in the rock. Therefore, in actual mining project, attention should be given to the changes in the water level around the shear stress concentrated regions. The height of the “CZ and WCFZ” in the plastic zone of the strike and dip planes are identical. After mining, in the range of 14.4 m above the roof of the coal seam shows complete failure, tensile failure occurs in the middle of the goaf, the surrounding area shows shear failure. With increases in the roof height to 14.4 m, the extent and form of the roof failure

gradually change. Tension failure above the goaf disappears and shear failure begins to dominate until the failure at 67.0 m of the roof disappears. Based on the size of the model and the variation of the plastic zones, it can be determined that the height of the CZ is about 14.4 m and the height of the WCFZ is about 67.0 m.

Figure 9 shows that there are two stress increasing areas in the coal pillars, the maximum stress is 14.7 MPa. This is because the stress increasing area at the cut hole is due to the slow release rate of strain energy stored in the coal body during the mining process, resulting in the accumulation of strain energy. The stress concentration at the end of the working face is due to the continuous advance of the working face, so it is too late to release the strain energy, which also causes the accumulation of strain energy. In order to further explore the results of the numerical simulation for determining the height of the “CZ and WCFZ”, five monitoring lines 1–1, 2–2, 3–3, 4–4 and 5–5 are drawn along the



(a) Strike plane of working face



(b) Dip plane of working face

Fig. 9 Distribution of vertical stress ahead of working face

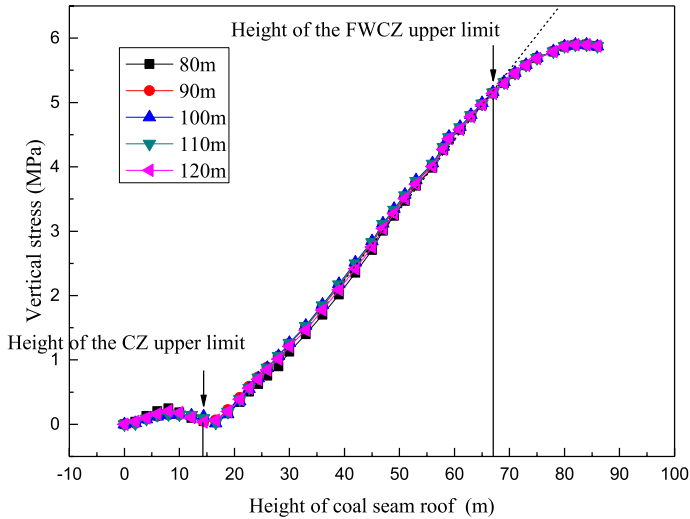


Fig. 10 Vertical stress in the rock versus distance above the roof at 80–120 m sections

goaf at 80 m, 90 m, 100 m, 110 m and 120 m, respectively along the strike direction to observe the changes in the vertical stress in the roof. Figure 10 shows the vertical stress above the roof for the sections at 80–120 m. It can be seen from the figure that the vertical stress in the rock above the roof initially increases slightly followed by a gradual decrease after 8.0 m until 14.4 m and then increases to 67.0 m and reaches the stress that is close to the original rock stress. Since the volume of rock will increase after it is broken, the height of the direct roof collapse accumulation is higher than its original height. Due to the fragmentation coefficient k_p , the upward support of the collapsed rock mass leads to the significant reduction of the vertical stress in the roof above 8.0 m. By analyzing the variations in the vertical stress in the roof, the height of the CZ at this working face is found to be 14.4 m and the height of the WCFZ is 67.0 m. Therefore, the height of the “CZ and WCFZ” can be preliminarily determined from the distribution and variation characteristics of the vertical stress above the goaf, which is basically consistent with the distribution of the plastic zone.

5 Identification of key stratum

To further explore the height of the WCFZ in the studied area, according to the key strata theory (Qian et al. 2003, 2011), the height of the WCFZ developed after mining is controlled by key stratum of the roof. Therefore, the development of the WCFZ should be related to the location of the key stratum in the overburden, and the height of the WCFZ can be further calculated from the key strata theory. Xu et al. (2009, 2012) thinks that traditional calculations of the height of the WCFZ are empirical based on statistical analyses of actual measurements. They only consider the influence of the lithology of the roof and thickness of the coal seam being mined, and ignore the controlling role of the movement of a key stratum in the overburden. Since the height of the WCFZ depends on specific geological conditions, neglecting geology will lead to errors in the

prediction of the WCFZ and possibly water intrusions in the mine. Therefore, identification of the key stratum can fully reflect the influence of the roof key stratum structure on the rock movement, and avoid the error caused by the results of mathematical statistics. Based on the conditions of the overburden strata in Working Face 23301, this paper applies the key strata theory to identify the location of a key stratum in determining the height of the WCFZ.

The key stratum is identified by the strength and stiffness of the rock. That is, the key stratum should have high elastic modulus, high strength and high bearing capacity calculated from:

$$q_1(X)|_n = E_1 h_1^3 \sum_{i=1}^n h_i r_i / \sum_{i=1}^n E_i h_i^3 \quad (1)$$

where h_i , r_i and E_i are the thickness, bulk density and elastic modulus of the i th hard rock layer respectively and $q_1(X)|_n$ is the load of the n th hard rock strata on the first hard rock stratum. Since the $n + 1$ th stratum is a hard rock, its deflection is less than that of the lower rock layer, and the upper layer does not require the lower layer to support its load; therefore it must have:

$$q_1(X)|_{n+1} < q_1(X)|_n \quad (2)$$

According to this stiffness criterion, only several harder strata will be found from the layers of overburden strata. However, this does not provide the sequence of breakage of the layers. The strength criterion is mainly based on comparing the broken distance of the hard strata to determine whether they break synchronously with breaking the key stratum in lower key stratum. The rock stratum is treated like a beam in calculating the strength criterion, and the limited span of the beam is equal to the maximum span that can be suspended with loading. The broken distance is the distance of coal mining when the rock stratum collapses. The distance considers the height of strata from coal seam and the fracture angle of strata. The final criterion in determining the key stratum is based on the value of the broken distance (Qian et al. 2003, 2011).

When calculating the limited span of a hard rock stratum, the fracture of a hard rock layer is basically a problem of plate breakage on elastic foundation, so to simplify the calculation, the limited span l_n of the n th hard rock layer can be calculated from the following formula:

$$l_n = h_n \sqrt{2\sigma_n/q_n} \quad (3)$$

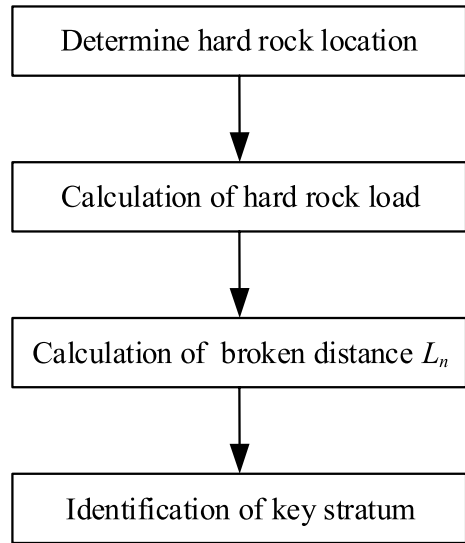
where l_n is the limited span (m), h_n is the thickness (m) of the rock layer, σ_n is the tensile strength (MPa) of the rock, q_n is the vertical stress (MPa) on the n th hard rock layer, and n is the total number of rock layers.

The location of the key stratum can be identified by considering the difference in suspension spacing between the upper and lower hard layers. The formula to calculate the broken distance L_n of the n th hard stratum is:

$$L_n = l_n + 2H_n \cot \gamma \quad (4)$$

where L_n is the broken distance of the hard rock stratum at the n th layer, l_n is the limited span of the hard rock layer at the n th layer, H_n is the distance of the hard rock layer at the n th layer from the top of the coal seam, and γ is the average broken angle of the rock layer.

Fig. 11 Flow chart of key stratum identification



Then, according to the discrimination principle (Qian et al. 2003, 2011), the broken distance of the rock stratum is compared to determine the location of the key stratum, and the main process is shown in Fig. 11.

The effect of the main key stratum on the development of WCFZ depends on the amount of space that allows rotation of the rock under the main key stratum. If the space available for rotation of the main key stratum is large, the subsidence of the blocks will increase, and the angle of rotation of the main key stratum will increase. This results in the transfer of the stresses carried by overlying rock block to the layer below, which will have a significant effect on the height of the WCFZ. If the space available for rotation of the main key stratum is small, the overburden stress can effectively be carried by the main key stratum, and the height of the WCFZ will not develop to the bedrock top of the main key stratum (Xu et al. 2009, 2012).

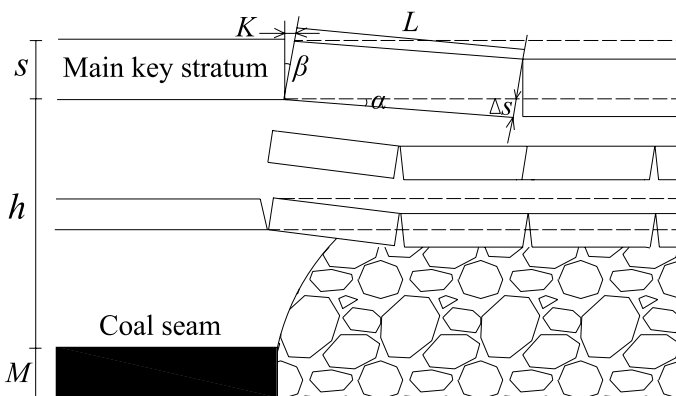


Fig. 12 Identification of main key stratum and fracture opening (Xu et al. 2009)

Table 3 Key stratum identification

No.	Distance from coal seam (m)	Thickness (m)	Type of rock	Key stratum location	Broken distance (m)	Limited span (m)
15	67	8	Siltstone	Main key stratum	60.81	24.91
2	10	11	Fine grained sandstone	Inferior key stratum	40.30	37.67
1	0	10	Medium grained sandstone	Inferior key stratum	39.88	39.88

Bold value indicates the key stratum position closest to the critical height 10M

Therefore, the calculation of the position of the main key stratum and the opening of fissures in the layer is developed, see Fig. 12, to find the critical distance to the main key stratum from the coal seam.

From Fig. 12:

$$\Delta s = M - h(k_p - 1) \quad (5)$$

$$\tan \beta = k/s \quad (6)$$

$$\tan \alpha = \Delta s/L \quad (7)$$

where Δs (m) is the maximum subsidence of the broken block in the main key stratum, M (m) is the thickness of the coal seam, h (m) is distance between the main key stratum and the top of the coal seam, k (m) is the opening of the crack in the main key stratum, s (m) is thickness of the main key stratum, L (m) is the broken block length, k_p is the fragmentation coefficient of layers below the main key stratum, β ($^\circ$) is the opening angle between the broken block and the main key stratum, and α ($^\circ$) is the change in angle before and after the broken block.

Since the values of α and β are the same, Eqs. (5), (6) and (7) are simplified and the following formula is obtained to calculate the fracture opening angle of the main key stratum:

$$k = [M - h(k_p - 1)]s/L \quad (8)$$

Assuming that the minimum broken crack opening of the main key stratum that forms WCFZ is k_m , the minimum distance h_m between the main key stratum and the coal seam can be calculated from Eq. (8) as:

$$h_m = [M - k_m(L/s)]/(k_p - 1) \quad (9)$$

Depending on the fracture condition of the roof key stratum after mining, the fracture opening angle of main key stratum is generally very small. Therefore by considering the fragmentation coefficient relative to the mining height $k_m(L/s)$ and the residual fragmentation coefficient k_p of rock strata below the main key stratum is generally 1.1–1.15, Eq. (9) is reduced to:

$$h_m = (7 - 10)M \quad (10)$$

The key stratum is divided into main key stratum and inferior key stratum. The location of the key stratum of the roof affects the height of the WCFZ. The fracture of the main key stratum will become part of the WCFZ only if the location of the main key stratum is less than a certain critical height from the coal seam and the overlying strata of the main key stratum will also become part of the WCFZ at the same time. When the main key stratum is within the critical height of $10M$ (10 times mined thickness), the WCFZ will extend to the top of the main key stratum. On the other hand, if the main key stratum lies beyond the critical height of $10M$, the WCFZ will extend to the bottom of the closest key stratum above the critical height of $10M$ (Xu et al. 2009, 2012). In the current case ($\gamma=75^\circ$), the results of determining the key stratum are summarized in Table 3.

The thickness of the coal seam (M) in the “CZ and WCFZ” borehole is 4 m, and the critical height of the key stratum calculated based on $10M$ is 40 m. The position of the key stratum closest to the critical height $10M$ is 67 m > 40 m from the coal seam height. Therefore, the height of the WCFZ should be calculated based on the position of the nearest key stratum that is above the critical height of 40 m which gives the height of the WCFZ of 67 m.

At the same time, the periodic weighting step can also be determined from the limited span of the key stratum. According to Eq. (11), the periodic weighting step l_{zn} can be calculated from:

$$l_{zn} = h_n \sqrt{\sigma_n / 3q_n} \quad (11)$$

Compared with the limited span from Eq. (3), the periodic weighting step from Eq. (11) is $\sqrt{6}/6$ times the limited span. The periodic weighting step of key stratum is 10.2–16.3 m, which is not very different from 14.0 to 17.0 m of the periodic weighting step based on coal mine compaction measurement. This shows the validity of the results from the determination of the key stratum, and also provides the basis for the prediction of the periodic weighting step of the coal mine working face.

6 Discussions

For the mining method of long wall free caving in China, the WCFZ mainly depends on the thicknesses of the mined seam, width of the working face, mined depth, dip angle of the coal seam and lithology characteristics of overburden strata. To study the influence of the above factors on the WCFZ of overburden strata, as shown in Table 4, the author collected 30 groups of measured data [16 groups of hard–hard, 5 groups of soft–hard (lower soft upper hard) and 9 groups of hard–soft (lower hard upper soft)], so as to carry out comparative analysis (Ma et al. 2008; Guo and Lou, 2019; Li et al. 2015; Yin et al. 2013).

It can be seen from Fig. 13a that with the increase of the thicknesses of the mined seam, the height of the WCFZ also increases. Moreover, when the thicknesses of the mined seam is the same, the height of WCFZ is hard–hard > hard–soft > soft–hard, which also shows that the lithology characteristics of overburden strata have a great influence on the WCFZ. As can be seen from Fig. 13b, the width of the working face is positively related to the height of WCFZ, but the influence is smaller than that of the thicknesses of the mined seam. However, the data points in Fig. 13c, d are relatively discrete and have no obvious regularity, which is because the influence of mined depth and dip angle of the coal seam on the WCFZ of overburden strata is smaller than the weight of thicknesses of the mined seam, width of the working face and lithology characteristics of overburden strata.

Table 4 Measured data of the WCFZ of roof overburden strata

No.	Working face	Thicknesses of the mined seam M (m)	Width of the working face L_x (m)	Mined depth H (m)	Dip angle of the coal seam α ($^\circ$)	Lithology characteristics of overburden strata	Height of the WCFZ H_{if} (m)	Height ratio of WCFZ to mined
1	Huafeng 1409	6.5	180	1024	32	Hard-hard	75.6	11.6
2	Nantun 63-10	5.8	154	400	6	Hard-hard	70.7	12.2
3	Fangezhuang first mining face (S)	1.9	70	173	20	Hard-hard	25.3	13.3
4	Liuhualing No. 4 coal seam	2.0	69	89	7	Hard-hard	45.9	23.0
5	Qilianta No. 1 coal seam	4.3	55	56	0	Hard-hard	42.5	9.9
6	Wangzhuang 6206 (1)	5.9	190	296	4	Hard-hard	114.7	19.4
7	Wangzhuang 6206 (2)	5.2	159	297	4	Hard-hard	102.3	19.7
8	Wangzhuang 6206 (3)	5.7	164	296	4	Hard-hard	114.9	20.2
9	Wuyang 7305 (1)	3.1	180	269	10	Hard-hard	65.4	21.1
10	Wuyang 7305 (2)	3.2	180	281	10	Hard-hard	74.8	23.4
11	Wuyang 7305 (3)	3.0	180	241	10	Hard-hard	59.9	20.0
12	Wuyang 7305 (4)	3.0	180	230	10	Hard-hard	61.0	20.3
13	Wuyang 7305 (5)	2.8	180	254	10	Hard-hard	63.9	22.8
14	Wuyang 7305 (6)	5.9	180	245	10	Hard-hard	70.0	11.9
15	Wuyang 7305 (7)	6.2	180	265	10	Hard-hard	90.0	14.5
16	Wuyang 7305 (8)	5.8	180	243	10	Hard-hard	91.7	15.8
17	Nantun 63	5.0	122	320	6	Soft-hard	67.7	13.5
18	Baodian 1314	7.5	174	367	6	Soft-hard	75.5	10.1
19	Xinji No. 2 1113107	5.1	149	475	28	Soft-hard	45.0	8.8
20	Xinji No. 1 1303	7.8	135	320	8	Soft-hard	83.9	10.8
21	Luxi 3-107	2.5	135	350	5	Soft-hard	20.0	8.0
22	Xinglongzhuang 1301	6.4	193	409	9	Hard-soft	72.9	11.4
23	Donghuantuo 2186	3.7	70	420	23	Hard-soft	56.8	15.4
24	Jining No. 3 1301	6.6	170	480	4	Hard-soft	67.9	10.3

Table 4 (continued)

No.	Working face	Thicknesses of the mined seam M (m)	Width of the working face L_x (m)	Mined depth H (m)	Dip angle of the coal seam α ($^\circ$)	Lithology characteristics of overburden strata	Height of the WCFZ H_{ii} (m)	Height ratio of WCFZ to mined
25	Qianjiaying 1672	3.0	143	484	17	Hard-soft	40.0	13.3
26	Yangzhuang No. 8 coal seam	1.7	65	320	6	Hard-soft	27.5	16.2
27	Xinglongzhuang 4320	8.0	170	450	8	Hard-soft	86.8	10.9
28	No. 3 coal seam of a mine	6.5	180	263	4	Hard-soft	83.9	12.9
29	Xinglongzhuang 2308	5.6	160	325	5	Hard-soft	51.5	9.2
30	Qidong No. 3 ₂ 41 coal seam	2.4	180	550	15	Hard-soft	55.3	23.0

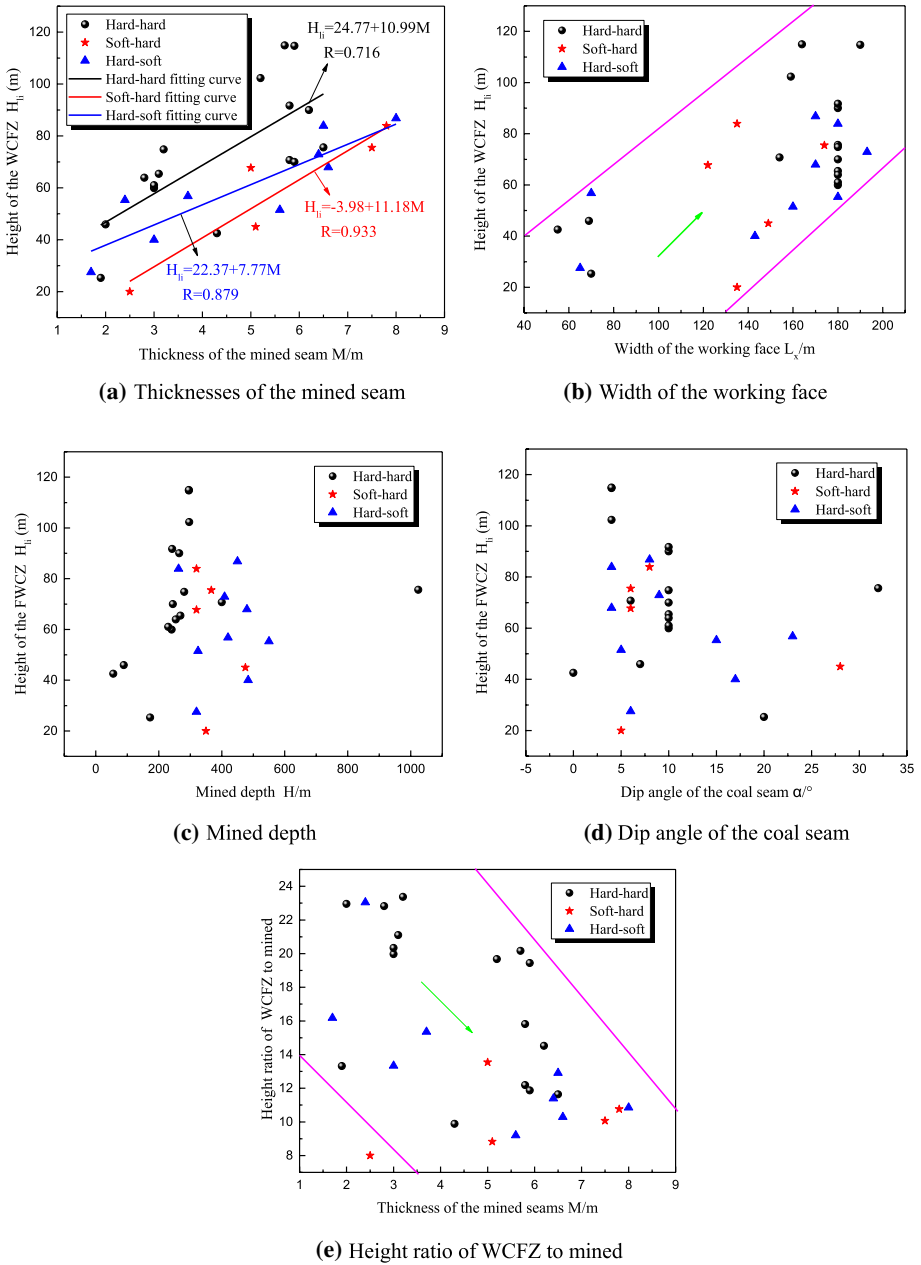


Fig. 13 Relationship between various factors and WCFZ

As shown in Fig. 13e, the height ratio of WCFZ to mined decreases with the increase of thicknesses of the mined seam. Through the above analysis, it is found that thicknesses of the mined seam, width of the working face and lithology characteristics of overburden strata are the main factors that affect the height of WCFZ.

Among the data in Table 4, the case where the lithology of overburden strata is hard–hard data is the most, and the data of other lithology characteristics of overburden strata is less. Based on this, only the lithology characteristics of overburden strata are fitted with multivariate linear regression according to the hard–hard data for thicknesses of the mined seam (M), width of the working face (L_x), and the height of WCFZ (H_{li}), and the formula for the height of hard–hard WCFZ is obtained ($R=0.81$).

$$H_{li} = 0.23L_x + 8.16M + 1.55 \quad (12)$$

The lithology characteristics of overburden strata of the working face in the study area is hard–hard, thicknesses of the mined seam is 4 m, width of the working face is 133 m, and the calculation result of Eq. (12) is 64.8 m. This result is basically consistent with the predicted WCFZ height of 67 m by numerical simulation and the key strata theory.

The WCFZ is the result of roof stress redistribution caused by mine pressure. Based on Fig. 13a, it can be seen that different lithologic combinations play an important role in the WCFZ. For homogeneous roof, the height of the WCFZ is positively related to the tensile strength. The harder the lithology of the overburden is, the more brittle the overburden is, the more likely it is to produce a WCFZ (Fig. 14a). However, the weaker the lithology of overburden strata is, the more creeping it is, the less likely it is to produce WCFZ. The fracture resistance of the hard and weak rock is better, so the height of the WCFZ is smaller than that of the hard–hard roof. For the hard–soft roof, the hard rock stratum is failed and the soft rock stratum must be affected (Fig. 14b). On the contrary, for the soft–hard roof, due to the strong plasticity of the soft rock, the obvious inhibition will reduce the secondary stress of mining, thus effectively reducing the degree of partial failure (Fig. 14c). Therefore, the height of the WCFZ with different mechanical structure types is different.

The harder the lithology of the roof is, the greater the development of the water-conducting fractured zone is. On the contrary, the harder the floor lithology is, the smaller the depth of floor failure is. At the same time, the lithology characteristics of the floor

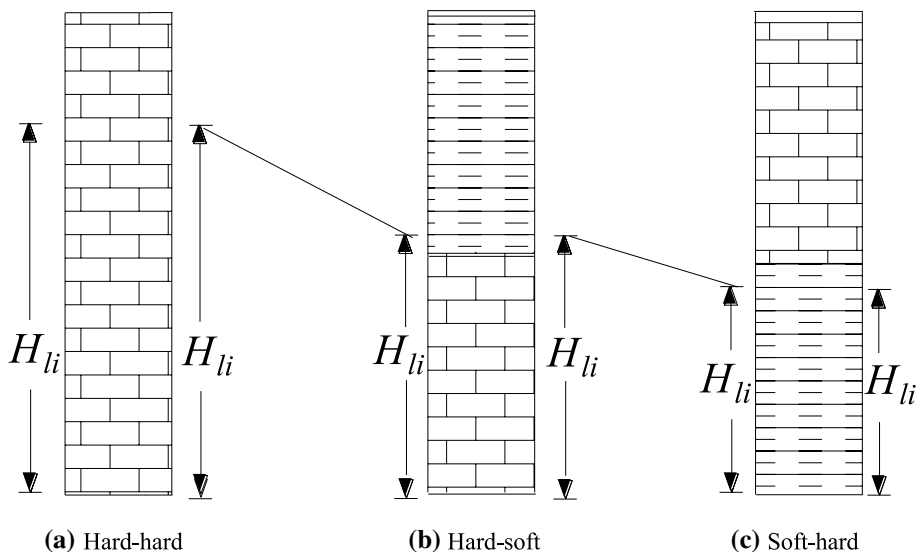


Fig. 14 Comparison of WCFZ of different lithology combinations of roof

also reflect this trend. The closer the hard rock is to the floor, the less the depth of floor failure is. The results show that the closer the hard rock is to the roof, the larger the water-conducting fractured zone is. This phenomenon of floor is also a kind of evidence for the characteristics of overburden strata.

7 Conclusions

Based on this study, the following conclusions are made:

- (1) The borehole imagery method is used to measure the borehole wall of the roof of Working Face 23301, and the height of the “CZ and WCFZ” is determined under the insufficient mining. The height of the CZ is found to be about 7.2 m and the height of the WCFZ is about 38.5 m.
- (2) In comparing the distribution of the plastic zone and the changes in the vertical stress in overburden strata with numerical simulation, it is found that the height of the “CZ and WCFZ” is about 14.4 m and 67.0 m, respectively. This effectively shows that the numerical model can capture the development of the “CZ and WCFZ”. The numerical model provides much more information than field observations, since as stress, size of the plastic zone, etc., which gives more insight into the process than based on field observations alone. Combining these two techniques can provide a more rational approach to improving the safety in long wall coal mining.
- (3) Based on the key strata theory and multiple linear regression, the height of the WCFZ in the working face is calculated to be 67.0 m and 64.8 m, respectively, which are close to the numerical simulation 67.0 m. These two methods can provide some guidance for predicting the height of the WCFZ. Moreover, based on the key strata theory, the periodic weighting step of the key stratum is found to be 10.2–16.3 m, which is similar to 14.0–17.0 m of the periodic weighting step of the coal mine based on compaction measurement. This method provides the basis for calculating the periodic weighting step for the coal mine working face. The application of this method also provides a new research idea for the determination of periodic weighting step in coal mines.
- (4) Through collecting 30 groups of measured data, the main factors affecting the WCFZ are analyzed. It is found that the thicknesses of the mined seam and lithology characteristics of overburden strata have the greatest influence on the WCFZ, followed by the width of the working face. With the increase of thicknesses of the mined seam, the height ratio of WCFZ to mined decreases gradually. For the different lithology characteristics of overburden strata, the height of WCFZ is hard–hard > hard–soft > soft–hard.
- (5) The comprehensive comparison of the four methods show that the height of the “CZ and WCFZ” measured in the field are both small, which also proves that it is the same that the roof is not fully caved during the test. However, numerical simulation, key strata theory and multiple linear regression can effectively make up for the lack of fully caved due to the limitations of field conditions. The combination of the four methods can provide a more reasonable basis for the determination of the height of the “CZ and WCFZ” in the study area. Therefore, the height of the “CZ and WCFZ” of the Working Face 23301 is 14.4 m and 64.8–67.0 m respectively.

Acknowledgments This research is supported by the Fundamental Research Funds for the Central Universities (Grant No. 2017CXNL03) and the Priority Academic Program Development of Jiangsu Higher

Education Institutions (PAPD). The authors are grateful to the anonymous reviewers for their helpful comments on the manuscript.

References

- Chen Y, Zhao GY, Wang SF et al (2019a) A case study on the height of a water-flow fracture zone above undersea mining: Sanshandao Gold Mine, China. *Environ Earth Sci* 78(4):122–137
- Chen Y, Zhu SY, Xiao SJ (2019b) Discussion on controlling factors of hydrogeochemistry and hydraulic connections of groundwater in different mining districts. *Nat Hazards* 99(2):689–704
- Fan LM, Ma XD (2018) A review on investigation of water-preserved coal mining in western China. *Int J Coal Sci Technol* 5(4):411–416
- Guo WB, Lou GZ (2019) Definition and distinguishing method of critical mining degree of overburden failure. *J China Coal Soc* 44(3):755–766 (in Chinese)
- Guo WB, Zou YF, Hou QL (2012) Fractured zone height of longwall mining and its effects on the overburden aquifers. *Int J Min Sci Technol* 22:603–606
- Guo WB, Zhao GB, Lou GZ et al (2019) A new method of predicting the height of the fractured water-conducting zone due to high-intensity longwall coal mining in China. *Rock Mech Rock Eng* 52(8):2789–2802
- Huang Z, Li XZ, Li SJ et al (2018) Investigation of the hydraulic properties of deep fractured rocks around underground excavations using high-pressure injection tests. *Eng Geol* 245:180–191
- Huang Z, Li SJ, Zhao K et al (2019) Estimating the hydraulic conductivity of deep fractured rock strata from high-pressure injection tests. *Mine Water Environ* 39:112–120
- Jia WY, Tian SY, Sun YT (2000) Imaging logging technology and its application. Petroleum Industry Press, Beijing (in Chinese)
- Li ZH, Xu YC, Li LF et al (2015) Forecast of the height of water flowing fractured zone based on BP neural networks. *J Min Saf Eng* 32(6):39–44 (in Chinese)
- Li HJ, Chen QT, Shu ZY et al (2018) On prevention and mechanism of bed separation water inrush for thick coal seams: a case study in China. *Environ Earth Sci* 77(22):759–771
- Liu XS, Tan YL, Ning JG et al (2015) The height of water-conducting fractured zones in longwall mining of shallow coal seams. *Geotech Geol Eng* 33(3):693–700
- Liu SL, Li WP, Wang QQ (2018) Height of the water-flowing fractured zone of the Jurassic coal seam in northwestern China. *Mine Water Environ* 37(2):312–321
- Liu WT, Pang LF, Liu YB et al (2019a) Characteristics analysis of roof overburden fracture in thick coal seam in deep mining and engineering application of super high water material in backfill mining. *Geotech Geol Eng* 37:2485–2494
- Liu ZG, Fan ZL, Zhang YJ (2019b) Fracture characteristics of overlying bedrock and clay aquiclude subjected to shallow coal seam mining. *Mine Water Environ* 38(1):136–147
- Ma YJ, Wu Q, Zhang ZY et al (2008) Research on prediction of water conducted fissure height in roof of coal mining seam. *Coal Sci Technol* 36(5):59–62 (in Chinese)
- Majidi A, Hassani FP, Nasiri MY (2012) Prediction of the height of distressed zone above the mined panel roof in longwall coal mining. *Int J Coal Geol* 98:62–72
- Miao XX, Cui XM, Wang JA et al (2011) The height of fractured water-conducting zone in undermined rock strata. *Eng Geol* 120:32–39
- Nan Z, Li J, Zhou W (2017) Study on the effect of fractures on conventional induction log based on physical and numerical simulation. *Acta Geod Geophys* 52(1):131–140
- Qian MG, Miao XX, Xu JL et al (2003) Key strata theory in ground control. China University of Mining and Technology Press, Xuzhou (in Chinese)
- Qian MG, Shi PW, Xu JL (2011) Mine pressure and strata control. China University of Mining and Technology Press, Xuzhou (in Chinese)
- Su BY, Yue JH (2017) Research of the electrical anisotropic characteristics of water-conducting fractured zones in coal seams. *Appl Geophys* 14(2):216–224
- Szokoli K, Szarka L, Metwally M et al (2018) Characterisation of a landslide by its fracture system using electric resistivity tomography and pressure probe methods. *Acta Geod Geophys* 53(1):15–30
- Wang FT, Tu SH, Zhang C et al (2016) Evolution mechanism of water-flowing zones and control technology for longwall mining in shallow coal seams beneath gully topography. *Environ Earth Sci* 75(19):1309–1325

- Wu Q, Shen JJ, Liu WT et al (2017) A RBFNN-based method for the prediction of the developed height of a water-conductive fractured zone for fully mechanized mining with sublevel caving. *Arab J Geosci* 10:172–181
- Wu Y, Huang Z, Zhao K et al (2020) Unsteady seepage solutions for hydraulic fracturing around vertical wellbores in hydrocarbon reservoirs. *Int J Hydrogen Energy* 45(16):9496–9503
- Xu JL, Wang XZ, Liu WT et al (2009) Effects of primary key stratum location on height of water flowing fracture zone. *Chin J Rock Mech Eng* 28(2):380–385 (in Chinese)
- Xu JL, Zhu WB, Wang XZ (2012) New method to predict the height of fractured water-conducting zone by location of key strata. *J China Coal Soc* 37(5):762–769 (in Chinese)
- Yin SX, Xu B, Xu H et al (2013) Study on calculation of height of water conducting fracture zone of coal seam roof under comprehensive mining conditions. *Coal Sci Technol* 41(9):138–142 (in Chinese)
- Zeng W, Huang Z, Wu Y et al (2020) Experimental investigation on mining-induced strain and failure characteristics of rock masses of mine floor. *Geomat Nat Hazards Risk* 11(1):491–509
- Zhang HQ, He YN, Tang CA et al (2009) Application of an improved flow-stress-damage model to the criticality assessment of water inrush in a mine: a case study. *Rock Mech Rock Eng* 42(6):911–930
- Zhang JX, Jiang HQ, Deng XJ et al (2014) Prediction of the height of the water-conducting zone above the mined panel in solid backfill mining. *Mine Water Environ* 33(4):317–326
- Zhang DY, Sui WH, Liu JW (2018a) Overburden failure associated with mining coal seams in close proximity in ascending and descending sequences under a large water body. *Mine Water Environ* 37(2):322–335
- Zhang Y, Cao SG, Guo S et al (2018b) Mechanisms of the development of water-conducting fracture zone in overlying strata during shortwall block backfill mining: a case study in Northwestern China. *Environ Earth Sci* 77(14):543–560